

A Computational Foray into the Formation and Reactivity of Metallabenzenes

Mark A. Iron,[†] André C. B. Lucassen,[†] Hagai Cohen,[‡] Milko E. van der Boom,^{*,†} and Jan M. L. Martin^{*,†}

Contribution from the Department of Organic Chemistry and Chemical Research Support Unit, Weizmann Institute of Science, 76100 Rehovot, Israel

Received May 17, 2004; E-mail: comartin@wicc.weizmann.ac.il; milko.vanderboom@weizmann.ac.il

Abstract: Various metallabenzene complexes, analogues of benzene where one CH unit has been replaced by an organometallic fragment, have been reported in the literature. A detailed theoretical investigation on the chemistry of these complexes is presented here. This includes an evaluation of their aromaticity, the mechanisms of formation of osmium, iridium, and platinum metallabenzene complexes, and one intriguing aspect of their chemistry, the formation of cyclopentadienyl (Cp) complexes. X-ray photoelectron spectroscopy (XPS) measurements on two osmabenzene examples are also presented. In addition, diffuse functions for use with the SDD and SDB-cc-pVDZ basis set-RECP combinations are presented for the transition metals.

Introduction

Faraday's 1825 discovery of benzene in the residue of London streetlamp oil¹ and Kekulé's proposal of its ringlike structure² sparked almost two centuries of intensive research into aromatic compounds and aromaticity. Research has included aromatic systems incorporating heteroatoms, such as the groups 14³ and 15⁴ analogues. One recent direction has been the introduction of transition metal complexes into the aromatic ring leading to metallabenzenes and related complexes (Scheme 1).^{5–33} Like-

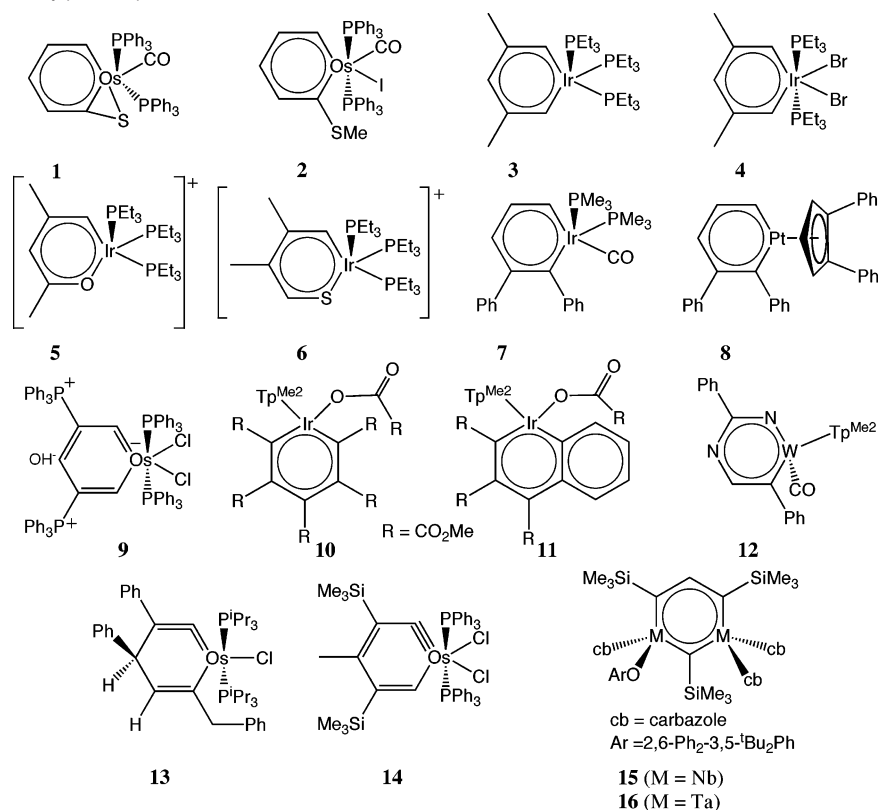
wise, metalloaromatic systems have also been implicated as intermediates in a number of reactions.^{34–37} Despite the significant amount of synthetic work, theoretical, kinetic, and mechanistic studies are relatively scarce.^{7,38,39} Recently, we reported on our computational studies into the cycloaddition reactivity of metallabenzenes toward acetone, CO₂, and CS₂^{40,41} and communicated our initial findings on their cyclopentadienyl (Cp) complex formation.⁴²

[†] Department of Organic Chemistry, Weizmann Institute of Science.

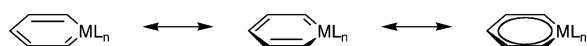
[‡] Chemical Research Support Unit, Weizmann Institute of Science.

- (1) Faraday, M. *Philos. Trans.* **1825**, *115*, 440–466.
- (2) Kekulé, A. *Bull. Soc. Chim.* **1864**, *3*, 98–110.
- (3) Tokitoh, N. *Acc. Chem. Res.* **2004**, *37*, 86–94.
- (4) Ashe, A. J., III. *Top. Curr. Chem.* **1982**, *105*, 125–155.
- (5) Bleeke, J. R. *Acc. Chem. Res.* **1991**, *24*, 271–277.
- (6) Bleeke, J. R. *Chem. Rev.* **2001**, *101*, 1205–1227.
- (7) Thorn, D. L.; Hoffmann, R. *Nouv. J. Chim.* **1979**, *3*, 39–45.
- (8) Elliott, G. P.; Roper, W. R.; Waters, J. M. *J. Chem. Soc., Chem. Commun.* **1982**, 811–813.
- (9) Rickard, C. E. F.; Roper, W. R.; Woodgate, S. D.; Wright, L. J. *J. Organomet. Chem.* **2001**, *623*, 109–115.
- (10) Bleeke, J. R.; Xie, Y.-F.; Peng, W.-J.; Chiang, M. *J. Am. Chem. Soc.* **1989**, *111*, 4118–4120.
- (11) Bleeke, J. R.; Behm, R.; Xie, Y.-F.; Clayton, T. W., Jr.; Robinson, K. D. *J. Am. Chem. Soc.* **1994**, *116*, 4093–4094.
- (12) Bleeke, J. R.; Behm, R.; Xie, Y.-F.; Chiang, M. Y.; Robinson, K. D.; Beatty, A. M. *Organometallics* **1997**, *16*, 606–623.
- (13) Bleeke, J. R.; Blanchard, J. M. B. *J. Am. Chem. Soc.* **1997**, *119*, 5443–5444.
- (14) Bleeke, J. R.; Blanchard, J. M. B.; Donnay, E. *Organometallics* **2001**, *20*, 324–336.
- (15) Bleeke, J. R.; Hinkle, P. V. *J. Am. Chem. Soc.* **1999**, *121*, 595–596.
- (16) Bleeke, J. R.; Hinkle, P. V. *Organometallics* **2001**, *20*, 1939–1951.
- (17) Gilbertson, R. D.; Weakley, T. J. R.; Haley, M. M. *J. Am. Chem. Soc.* **1999**, *121*, 2597–2598.
- (18) Gilbertson, R. D.; Weakley, T. J. R.; Haley, M. M. *Chem. Eur. J.* **2000**, *6*, 437–441.
- (19) Gilbertson, R. D.; Lau, T. L. S.; Lanza, S.; Wu, H.-P.; Weakley, T. J. R.; Haley, M. M. *Organometallics* **2003**, *22*, 3279–3289.
- (20) Jacob, V.; Weakley, T. J. R.; Haley, M. M. *Angew. Chem., Int. Ed.* **2002**, *41*, 3470–3473.
- (21) Landorf, C. W.; Jacob, V.; Weakley, T. J. R.; Haley, M. M. *Organometallics* **2004**, *23*, 1174–1176.
- (22) Paneque, M.; Posadas, C. M.; Poveda, M. L.; Rendón, N.; Salazar, V.; Oñate, E.; Mereiter, K. *J. Am. Chem. Soc.* **2003**, *125*, 9898–9899.
- (23) Xia, H.; He, G.; Zhang, H.; Wen, T. B.; Sung, H. H. Y.; Williams, I. D.; Jia, G. *J. Am. Chem. Soc.* **2004**, *126*, 6862–6863.
- (24) Feng, S. G.; White, P. S.; Templeton, J. L. *Organometallics* **1993**, *12*, 1765–1774.
- (25) Bianchini, C.; Meli, A.; Peruzzini, M.; Vizza, F.; Frediani, P.; Herrera, V.; Sanchez-Delgado, R. A. *J. Am. Chem. Soc.* **1993**, *115*, 2731–2742.
- (26) Chen, J.; Daniels, L. M.; Angelici, R. J. *J. Am. Chem. Soc.* **1990**, *112*, 199–204.
- (27) Barrio, P.; Esteruelas, M. A.; Oñate, E. *J. Am. Chem. Soc.* **2004**, *126*, 1946–1947.
- (28) Wen, T. B.; Zhou, Z. Y.; Jia, G. *Angew. Chem., Int. Ed.* **2001**, *40*, 1951–1954.
- (29) Wen, T. B.; Ng, S. M.; Hung, W. Y.; Zhou, Z. Y.; Lo, M. F.; Shek, L.-Y.; Williams, I. D.; Lin, Z.; Jia, G. *J. Am. Chem. Soc.* **2003**, *125*, 884–885.
- (30) Ng, S. M.; Huang, X.; Wen, T. B.; Jia, G.; Lin, Z. *Organometallics* **2003**, *22*, 3898–3904.
- (31) Roper, W. R. *Angew. Chem., Int. Ed.* **2001**, *40*, 2440–2441.
- (32) Profilet, R. D.; Fanwick, P. E.; Rothwell, I. P. *Angew. Chem., Int. Ed. Engl.* **1992**, *31*, 1261–1263.
- (33) Riley, P. N.; Profilet, R. D.; Salberg, M. M.; Fanwick, P. E.; Rothwell, I. P. *Polyhedron* **1998**, *17*, 773–779.
- (34) Schrock, R. R.; Pedersen, S. F.; Churchill, M. R.; Ziller, J. W. *Organometallics* **1984**, *3*, 1574–1583.
- (35) Hughes, R. P.; Trujillo, H. A.; Rheingold, A. L. *J. Am. Chem. Soc.* **1993**, *115*, 1583–1585.
- (36) Hughes, R. P.; Trujillo, H. A.; Egan, J. W., Jr.; Rheingold, A. L. *J. Am. Chem. Soc.* **2000**, *122*, 2261–2271.
- (37) Chin, R. M.; Jones, W. D. *Angew. Chem., Int. Ed. Engl.* **1992**, *31*, 357–358.
- (38) Chamizo, J. A.; Morgado, J.; Sosa, P. *Organometallics* **1993**, *12*, 5005–5007.
- (39) Masui, H. *Coord. Chem. Rev.* **2001**, *219–221*, 957–992.
- (40) Iron, M. A.; Martin, J. M. L.; van der Boom, M. E. *Chem. Commun.* **2003**, 132–133.
- (41) Iron, M. A.; Martin, J. M. L.; van der Boom, M. E. *J. Am. Chem. Soc.* **2003**, *125*, 11702–11709.

Scheme 1. Literature Examples of Isolated Metallabenzenes (**1–4**, **7–10**) and Related Compounds (**5**, **6**, **11–16**, $\text{Tp}^{\text{Me}_2} = \text{Hydrotris(3,5-dimethylpyrazolyl)Borate}$)^{8–24,27–33}



Scheme 2. Resonance Structures of Metallabenzenes



In light of all these studies, it is remarkable that the question of the formal metal oxidation state of these intriguing complexes is still not resolved.¹² If one considers the metallabenzene in one of its Kekulé structures (Scheme 2), the organic fragment can be considered to consist of a vinyl and a carbene ligand. The former is a two-electron anionic ligand. The latter, however, can be either a Fischer⁴³ or a Schrock⁴⁴ type carbene. A Fischer carbene, which generally is considered to be a carbene with a heteroatom or other π -donor,^{45,46} is a two-electron neutral ligand leading to an overall four-electron monoanionic organic fragment in the metallabenzene. Under such a scheme, complexes **3** and **7**, for example, would formally be Ir(I) complexes (see Supporting Information, Table S1). A Schrock carbene, which is also known as an alkylidene complex and is generally considered to be a carbene with only C and/or H substituents and no π -donor,^{45,46} is a four-electron dianionic ligand. In this case, the metallabenzene organic fragment would be a six-electron trianionic ligand and complexes **3** and **7** would be formally Ir(III) complexes. One may observe that the effect of resonance would make the rest of the ring a π -acceptor, rather than a π -donor, vis-à-vis the carbene moiety.

In this paper, we report on the formation, stability, and reactivity of Os, Ru, Fe, Ir, Rh, Pt, Pd, and Re metallabenzenes and on the question of the formal metal oxidation state. First, we will in brief consider the question of aromaticity of these complexes. To this end, we will examine the geometrical parameters of the metallabenzene complexes, their molecular orbitals, calculated nuclear independent chemical shifts (NICS) and magnetic susceptibility anisotropies ($\Delta\chi$), and reactivities. Next, the computed mechanism that we found for the formation of the Os, Ir, and Pt metallabenzenes **1**, **7**, and **8** will be discussed. Furthermore, a full account of the Cp formation reactivity will be presented along with the salient points of the cycloaddition reactivity of iridium-based metallabenzenes.^{40,41} In addition, the results of X-ray photoelectron spectroscopy (XPS) on complexes **1** and **2** will be presented.

Experimental Details

The osmabenzene **1** and **2** were prepared according to literature procedures^{47,48} starting from commercially available (Sigma-Aldrich) ammonium hexachloroosmate, $(\text{NH}_4)_2\text{OsCl}_6$. The identity and purity of **1** were determined by ^1H and $^{31}\text{P}\{^1\text{H}\}$ NMR,^{47,48} UV-vis spectroscopy, and X-ray photoelectron spectroscopy (XPS). XPS measurements were carried out with an AXIS-HS Kratos setup, using a monochromatized Al K α X-ray source ($h\nu = 1486.6$ eV) and pass energies ranging from 20 to 80 eV. The energy scale was calibrated referring to the C 1s line at 284.7 eV.⁴⁹ The spectrum of **1** was measured as a powder on double-sided carbon tape, while **2** was measured drop-casted on an oxidized silicon surface.

(42) Iron, M. A.; Martin, J. M. L.; van der Boom, M. E. *J. Am. Chem. Soc.* **2003**, *125*, 13020–13021.

(43) Fischer, E. O.; Maasböl, A. *Angew. Chem., Int. Ed. Engl.* **1964**, *3*, 580–581.

(44) Schrock, R. R. *J. Am. Chem. Soc.* **1974**, *96*, 6796–6797.

(45) Frenking, G.; Fröhlich, N. *Chem. Rev.* **2000**, *100*, 717–774.

(46) Collman, J. P.; Hegedus, L. S.; Norton, J. R.; Finke, R. G. *Principles and Applications of Organotransition Metal Chemistry*; University Science Books: Mill Valley, CA, 1987.

(47) Elliott, G. P.; McAuley, N. M.; Roper, W. R. *Inorg. Synth.* **1989**, *26*, 184–189.

(48) Rickard, C. E. F.; Roper, W. R.; Woodgate, S. D.; Wright, L. J. *Angew. Chem., Int. Ed.* **2000**, *39*, 750–752.

(49) *Handbook of X-ray Photoelectron Spectroscopy*; Chastain, J., Ed.; Perkin-Elmer: Eden Prairie, MN, 1992.

Computational Details

Unless otherwise noted, all calculations were carried out using Gaussian 98 revision A11.⁵⁰ The mPW1K (modified Perdew-Wang 1-parameter for kinetics) DFT exchange-correlation functional of Truhlar and co-workers⁵¹ was used to investigate the reactions. This functional is based on the Perdew–Wang exchange functional⁵² with Adamo and Barone’s modified enhancement factor⁵³ and the Perdew–Wang correlation functional.⁵² A larger percentage of Hartree–Fock exchange is introduced into the functional⁵¹ to circumvent the underestimated barrier heights typical of standard exchange-correlation functionals. It has been shown (e.g., refs 51, 54–56) that this functional generally yields much more reliable reaction barrier heights than B3LYP or other “conventional” exchange-correlation functionals.

With this functional, two basis set-RECP (relativistic effective core potential) combinations were used. The first, denoted SDD, is the combination of the Huzinaga–Dunning double- ζ basis set on lighter elements with the Stuttgart–Dresden basis set-RECP combination⁵⁷ on transition metals. The second, denoted SDB-cc-pVDZ, combines the Dunning cc-pVDZ basis set⁵⁸ on the main group elements and the Stuttgart–Dresden basis set-RECP on the transition metals with an added f -type polarization exponent taken as the geometric average of the two f -exponents given in the Appendix to ref 59. Geometry optimizations were carried out using the former basis set while the energetics of the reaction were calculated at these geometries with the latter basis set; this level of theory is conventionally denoted as mPW1K/SDB-cc-pVDZ//mPW1K/SDD.

Since Gaussian 98 uses the same number of radial grid points throughout the periodic table, the “ultrafine” grid, i.e., a pruned (99,590) grid, was used throughout the calculations as recommended in ref 60. Nonetheless, in the case of *trans,cis*-[(C₅H₅Ir)(PH₃)₂(CH₃CN)₂]²⁺ (**21**), even the denser grids were insufficient and a persistent, very small imaginary frequency (6i cm⁻¹) was obtained. This was however ignored as a grid artifact. Regardless, this imaginary frequency corresponds to rotation around NC–CH₃ bonds, which should be nearly free.

The identities of the transition states were confirmed by having only one imaginary vibrational mode suitable for the desired reaction. In addition, an intrinsic reaction coordinate (IRC) calculation was performed on each transition state to confirm connectivity with the reactant(s) and the product.^{61–63} Due to the length of the IRC calculation, the default pruned (75,302) grid was used, and it is not expected that this will have any significant impact on the IRC calculation.

Bulk solvation effects⁶⁴ were approximated using a polarized continuum (overlapping spheres) model (PCM).^{65–67} The solvent used in the calculations, be it diethyl ether ($\epsilon = 4.335$), toluene ($\epsilon = 2.379$), heptane ($\epsilon = 1.92$), methylene chloride ($\epsilon = 8.93$), or acetonitrile ($\epsilon = 36.64$), was generally the same as that used in the relevant experimental systems; in some cases diethyl ether has been used instead of tetrahydrofuran or toluene instead of benzene, but the impact of these substitutions should be insignificant.

For interpretation purposes, natural population analysis (NPA) charges⁶⁸ were derived from the natural bond order (NBO) analysis⁶⁸ at the mPW1K/SDD level of theory. Atomic polar tensor (APT) charges⁶⁹ were derived from the mPW1K/SDD analytical second derivatives (vibrational frequencies) calculation. Molecular orbitals were visualized using GaussView.⁷⁰

Nucleus-independent chemical shifts (NICS)^{71,72} and magnetic susceptibility anisotropies ($\Delta\chi$) were calculated at the B97-1/aug-SDB-cc-pVDZ level of theory using Gaussian 03 rev. B02.⁷³ The B97-1 exchange-correlation functional⁷⁴ is Handy and co-workers’ reparameterization of Becke’s B97 functional.⁷⁵ The aug-SDB-cc-pVDZ basis set is similar to the abovementioned SDB-cc-pVDZ basis set but uses Dunning’s aug-cc-pVDZ basis set on the main group elements^{76,77} and an additional *spdf* set of diffuse functions of the metal center, which are listed in Table S2 (Supporting Information); for more details on the development of the basis set, see the Results section. The NMR chemical shifts and magnetic susceptibility tensors (χ) were calculated using the gauge-independent atomic orbital (GIAO) method,^{78–82} the NICS with a “dummy” atom suspended either 0.0 or 1.0 Å above the center of the ring. The magnetic susceptibility anisotropy ($\Delta\chi$) is defined accordingly:

$$\Delta\chi = \chi_{zz} - (\frac{1}{2})(\chi_{xx} + \chi_{yy}) \quad (1)$$

where the z -axis is defined as perpendicular to the plane of the metallabenzene ring.⁸³

- (50) Frisch, M. J.; Trucks, G. W.; Schlegel, H. B.; G. E. Scuseria; Robb, M. A.; Cheeseman, J. R.; Zakrzewski, V. G.; Montgomery, J. A., Jr.; Stratmann, R. E.; Burant, J. C.; Dapprich, S.; Millam, J. M.; Daniels, A. D.; Kudin, K. N.; Strain, M. C.; Farkas, O.; Tomasi, J.; Barone, V.; Cossi, M.; Cammi, R.; Mennucci, B.; Pomelli, C.; Adamo, C.; Clifford, S.; Ochterski, J.; Petersson, G. A.; Ayala, P. Y.; Cui, Q.; Morokuma, K.; Salvador, P.; Dannenberg, J. J.; Malick, D. K.; Rabuck, A. D.; Raghavachari, K.; Foresman, J. B.; Cioslowski, J.; Ortiz, J. V.; Baboul, A. G.; Stefanov, B. B.; Liu, G.; Liashenko, A.; Piskorz, P.; Komaromi, I.; Gomperts, R.; Martin, R. L.; Fox, D. J.; Keith, T.; Al-Laham, M. A.; Peng, C. Y.; Nanayakkara, A.; Challacombe, M.; Gill, P. M. W.; Johnson, B.; Chen, W.; Wong, M. W.; Andres, J. L.; Gonzalez, C.; Head-Gordon, M.; Replogle, E. S.; Pople, J. A. *Gaussian 98*, Revision A.11; Gaussian Inc.: Pittsburgh, PA, 2001.
- (51) Lynch, B. J.; Fast, P. L.; Harris, M.; Truhlar, D. G. *J. Phys. Chem. A* **2000**, *104*, 4811–4815.
- (52) Perdew, J. P.; Chevary, J. A.; Vosko, S. H.; Jackson, K. A.; Perderson, M. R.; Singh, D. J.; Fiolhais, C. *Phys. Rev. B* **1992**, *46*, 6671–6687.
- (53) Adamo, C.; Barone, V. *J. Chem. Phys.* **1998**, *108*, 664–675.
- (54) Lynch, B. J.; Truhlar, D. G. *J. Phys. Chem. A* **2001**, *105*, 2936–2941.
- (55) Parthiban, S.; de Oliveira, G.; Martin, J. M. L. *J. Phys. Chem. A* **2001**, *105*, 895–904.
- (56) Iron, M. A.; Lo, H. C.; Martin, J. M. L.; Keinan, E. *J. Am. Chem. Soc.* **2002**, *124*, 7041–7054.
- (57) Dolg, M. In *Modern Methods and Algorithms of Quantum Chemistry*; Grotendorst, J., Ed.; John von Neumann Institute for Computing: Jülich, 2000; Vol. 1, pp 479–508.
- (58) Dunning, T. H., Jr. *J. Chem. Phys.* **1989**, *90*, 1007–1023.
- (59) Martin, J. M. L.; Sundermann, A. *J. Chem. Phys.* **2001**, *114*, 3408–3420.
- (60) Martin, J. M. L.; Bauschlicher, C. W., Jr.; Ricca, A. *Comput. Phys. Commun.* **2001**, *133*, 189–201.
- (61) Fukui, K. *Acc. Chem. Res.* **1981**, *14*, 363–368.
- (62) Gonzalez, C.; Schlegel, H. B. *J. Chem. Phys.* **1989**, *90*, 2154–2161.
- (63) Gonzalez, C.; Schlegel, H. B. *J. Phys. Chem.* **1990**, *94*, 5523–5527.
- (64) Cramer, C. J. *Essentials of Computational Chemistry: Theories and Models*; John Wiley & Sons: Chichester, U.K., 2002; pp 347–383.
- (65) Miertus, S.; Scrocco, E.; Tomasi, J. *Chem. Phys.* **1981**, *55*, 117.
- (66) Miertus, S.; Tomasi, J. *Chem. Phys.* **1982**, *65*, 239.
- (67) Cossi, M.; Barone, V.; Cammi, R.; Tomasi, J. *Chem. Phys. Lett.* **1996**, *255*, 327–335.
- (68) Reed, A. E.; Curtiss, L. A.; Weinhold, F. *Chem. Rev.* **1988**, *88*, 899–926.
- (69) Cioslowski, J. *J. Am. Chem. Soc.* **1989**, *111*, 8333–8336.
- (70) GaussView 3.0; Gaussian Inc.: Pittsburgh, PA, 2003.
- (71) Schleyer, P. v. R.; Maerker, C.; Dransfeld, A.; Jiao, H.; van Eikema Hommes, N. J. R. *J. Am. Chem. Soc.* **1996**, *118*, 6317–6318.
- (72) Schleyer, P. v. R.; Jiao, H.; van Eikema Hommes, N. J. R.; Malkin, V. G.; Malkina, O. L. *J. Am. Chem. Soc.* **1997**, *119*, 12669–12670.
- (73) Frisch, M. J.; Trucks, G. W.; Schlegel, H. B.; Scuseria, G. E.; Robb, M. A.; Cheeseman, J. R.; Montgomery, J. A., Jr.; Vreven, T.; Kudin, K. N.; Burant, J. C.; Millam, J. M.; Iyengar, S. S.; Tomasi, J.; Barone, V.; Mennucci, B.; Cossi, M.; Scalmani, G.; Rega, N.; Petersson, G. A.; Nakatsuji, H.; Hada, M.; Ehara, M.; Toyota, K.; Fukuda, R.; Hasegawa, J.; Ishida, M.; Nakajima, T.; Honda, Y.; Kitao, O.; Nakai, H.; Klene, M.; Li, X.; Knox, J. E.; Hratchian, H. P.; Cross, J. B.; Adamo, C.; Jaramillo, J.; Gomperts, R.; Stratmann, R. E.; Yazyev, O.; Austin, A. J.; Cammi, R.; Pomelli, C.; Ochterski, J. W.; Ayala, P. Y.; Morokuma, K.; Voth, G. A.; Salvador, P.; Dannenberg, J. J.; Zakrzewski, V. G.; Dapprich, S.; Daniels, A. D.; Strain, M. C.; Farkas, O.; Malick, D. K.; Rabuck, A. D.; Raghavachari, K.; Foresman, J. B.; Ortiz, J. V.; Cui, Q.; Baboul, A. G.; Clifford, S.; Cioslowski, J.; Stefanov, B. B.; Liu, G.; Liashenko, A.; Piskorz, P.; Komaromi, I.; Martin, R. L.; Fox, D. J.; Keith, T.; Al-Laham, M. A.; Peng, C. Y.; Nanayakkara, A.; Challacombe, M.; Gill, P. M. W.; Johnson, B.; Chen, W.; Wong, M. W.; Gonzalez, C.; and Pople, J. A. *Gaussian 03*, Revision B.02; Gaussian, Inc.: Pittsburgh, PA, 2003.
- (74) Hamprecht, F. A.; Cohen, A. J.; Tozer, D. J.; Handy, N. C. *J. Chem. Phys.* **1998**, *109*, 6264–6271.
- (75) Becke, A. D. *J. Chem. Phys.* **1997**, *107*, 8554–8560.
- (76) Woon, D. E.; Dunning, T. H., Jr. *J. Chem. Phys.* **1993**, *98*, 1358–1371.
- (77) Kendall, R. A.; Dunning, T. H., Jr.; Harrison, R. J. *J. Chem. Phys.* **1992**, *96*, 6796–6806.
- (78) London, F. *J. Phys. Radium, Paris* **1937**, *8*, 397.
- (79) McWeeny, R. *Phys. Rev.* **1962**, *126*, 1028–1034.
- (80) Ditchfield, R. *Mol. Phys.* **1974**, *27*, 789.
- (81) Dodds, J. L.; McWeeny, R.; Sadlej, A. J. *Mol. Phys.* **1980**, *41*, 1419.
- (82) Wolinski, K.; Hinton, J. F.; Pulay, P. *J. Am. Chem. Soc.* **1990**, *112*, 8251–8260.

In this study, model systems are used to represent the larger experimental system. Substituents on the ring or on the phosphine ligands are often replaced by hydrogen atoms. This is not expected to significantly affect the results unless there is a major steric contribution. This was confirmed here for the preparation of complex **50** (vide infra, Scheme 4) where the impact of adding two methyl groups on the metallabenzene ring was found to be insignificant. Previously, we verified that using PMe_3 ligands instead of PH_3 on metallabenzene systems resulted in only minor changes.⁴¹

Results and Discussion

aug-SDB-cc-pVDZ Basis Sets. To evaluate the magnetic properties, suitable basis sets are required for the GIAO NMR calculation. As the effects include regions of space distant from the nuclei, it is reasonable that diffuse functions will be needed in the basis set. For that reason, the cc-pVDZ basis set on the 1st and 2nd row elements in the SDB-cc-pVDZ basis set was replaced by its augmented version. However, diffuse functions were required for the SDB basis set-RECP combination used on the transition metals. As the highest angular momentum function in the basis set is f , a set of diffuse $spdf$ functions is required.

The basis set completeness profile of Chong provides an efficient means of generating diffuse s , p , and d functions for any element for any basis set.⁸⁴ This method involves using a test Gaussian type orbital $G(\xi)$ to scan space and plot the sum of squares of the overlap

$$Y(\xi) = \sum_m \langle G(\xi) | \psi_m \rangle \langle \psi_m | G(\xi) \rangle$$

between the basis set

$$\psi_j = \sum_i \phi_i c_{ij}$$

and $G(\xi)$ as a function of $\log(\xi)$. The diffuse exponents were determined by searching for the exponent ξ such that

$$\langle G(\xi) | G(2.5\xi) \rangle \langle G(2.5\xi) | G(\xi) \rangle = Y(\xi)$$

The exponent was determined by a grid search followed by Newton–Raphson. In such a manner, the $spdf$ diffuse functions can be readily obtained using a simple code written by Chong.⁸⁴

The f functions were optimized using a code written in house for basis set optimizations.⁸⁵ The f function was optimized on top of the SDB plus diffuse $spdf$ basis set-RECP combination. Either the electron affinity ($M^- - M^0$) or the energy of the anion was minimized at the CISD level with full spatial and spin symmetry imposed using the MOLPRO 2000.1 ab initio program⁸⁶ to obtain the diffuse f function. The choice between the electron affinity and the energy of the anion was made based on which of the two had better convergence behavior. To determine whether a reasonable exponent was obtained, η_f was plotted

versus z^* (the atomic number of the element less the number of electrons included in the RECP, 10 for 1st row transition metals, 28 for 2nd row, and 60 for 3rd row). It was expected that the exponents, within each row, should follow a regular pattern. It was found that the exponents best fit a power function. The f functions for Zn, Cd, and Hg, which do not have stable anions, were determined by extrapolation using the obtained power fit. The sets of diffuse $spdf$ exponents thus obtained for the transition metals and the parameters of the power fits found are listed in the Supporting Information (Table S2 and S3).

Metallabenzene Aromaticity. The question of aromaticity^{87–93} is a difficult one to address and often considered philosophical, or even contentious, in nature.^{89,93} There are a number of criteria that are commonly used to evaluate the aromaticity of a system, including resonance energy, structure, electronic structure, magnetic resonance, and reactivity.^{87,89–93} The resonance energy criterion is not as straightforward to evaluate as the others. Here, we examine various metallabenzene complexes to evaluate the aromatic nature of these systems. The methods used are generally applied to organic systems, although it is reasonable that they will also be applicable to these organometallic species.

The structural criteria of aromatic systems are probably the easiest to evaluate.^{87,90,91} The system should involve planar rings with bonds of equal length intermediate between single and double carbon–carbon bonds. The closer the bond lengths are to alternating single and double bonds, the less aromatic the system is. Metallabenzenes are observed, both experimentally^{8,12,17–22,94,95} and computationally, to be planar and to have C–C and M–C bond lengths intermediate between single and double bonds. Table S4 (Supporting Information) lists the ring bond lengths in a number of computational systems (**17–34**). One can clearly observe, based on the planar structure with bond-length equalization, that these systems are aromatic. In fact, in a number of systems, the two M–C_{ortho}, C_{ortho}–C_{meta} and C_{meta}–C_{para} bonds are of equal, or nearly equal, lengths. The bonds vary significantly only in the nonsymmetric systems and this is most likely due to other effects, most notably the different trans effects of the different ligands (CO, PR₃, halides). These M–C bond lengths (1.9–2.1 Å, Table S4) are on the border between experimentally determined M–C and M=C bond lengths in other systems (Table S5, Supporting Information). Also listed in Table S4 are the sums of the internal ring angles ($\Sigma\angle$) in these systems, which are very close to 720°, the sum in a hexagon. In a similar fashion, the ring dihedral angles are all very small, and in a number of cases, all six dihedral angles are 0.00°. The largest deviations, both in $\Sigma\angle$ and in the dihedral angles, occur in the cases where the metallabenzenes are less stable toward Cp formation (vide infra).

The electronic structure of metallabenzenes also supports an aromatic nature. Figure 1 depicts the aromatic molecular orbitals (MO's) of benzene and selected ones of $(\text{C}_5\text{H}_5\text{Ir})(\text{PH}_3)_3$ (**17**), $(\text{C}_5\text{H}_5\text{Pt})\text{Cp}$ (**18**), and $[(\text{C}_5\text{H}_5\text{Pt})(\text{PH}_3)_2]^+$ (**26**). All the metallabenzenes studied have similar molecular orbitals, although the

(83) In Gaussian 03, it is required to set IOp(10/6=1) to have the magnetic susceptibility tensors (χ) calculated and printed to the log file.

(84) Chong, D. P. *Can. J. Chem.* **1995**, *73*, 79–83.

(85) Iron, M. A.; Oren, M.; Martin, J. M. L. *Mol. Phys.* **2003**, *101*, 1345–1361.

(86) MOLPRO is a package of ab initio programs written by Werner, H.-J. and Knowles, P. J., with contributions from Amos, R. D.; Bernhardtsson, A.; Berning, A.; Celani, P.; Cooper, D. L.; Deegan, M. J. O.; Dobbyn, A. J.; Eckert, F.; Hampel, C.; Hetzer, G.; Korona, T.; Lindh, R.; Lloyd, A. W.; McNicholas, S. J.; Manby, F. R.; Meyer, W.; Mura, M. E.; Nicklass, A.; Palmieri, P.; Pitzer, R.; Rauhut, G.; Schütz, M.; Stoll, H.; Stone, A. J.; Tarroni, R.; Thorsteinsson, T.

(87) Schleyer, P. v. R.; Jiao, H. *Pure Appl. Chem.* **1996**, *68*, 209–218.

(88) Schleyer, P. v. R. *Chem. Rev.* **2001**, *101*, 1115–1117.

(89) Gomes, J. A. N. F.; Mallion, R. B. *Chem. Rev.* **2001**, *101*, 1349–1383.

(90) Krygowski, T. M.; Cyrański, M. K. *Chem. Rev.* **2001**, *101*, 1385–1419.

(91) Katritzky, A. R.; Jug, K.; Oniciu, D. C. *Chem. Rev.* **2001**, *101*, 1421–1449.

(92) De Prof, F.; Geerlings, P. *Chem. Rev.* **2001**, *101*, 1451–1464.

(93) Balaban, A.; Oniciu, D. C.; Katritzky, A. R. *Chem. Rev.* **2004**, *104*, 2777–2812.

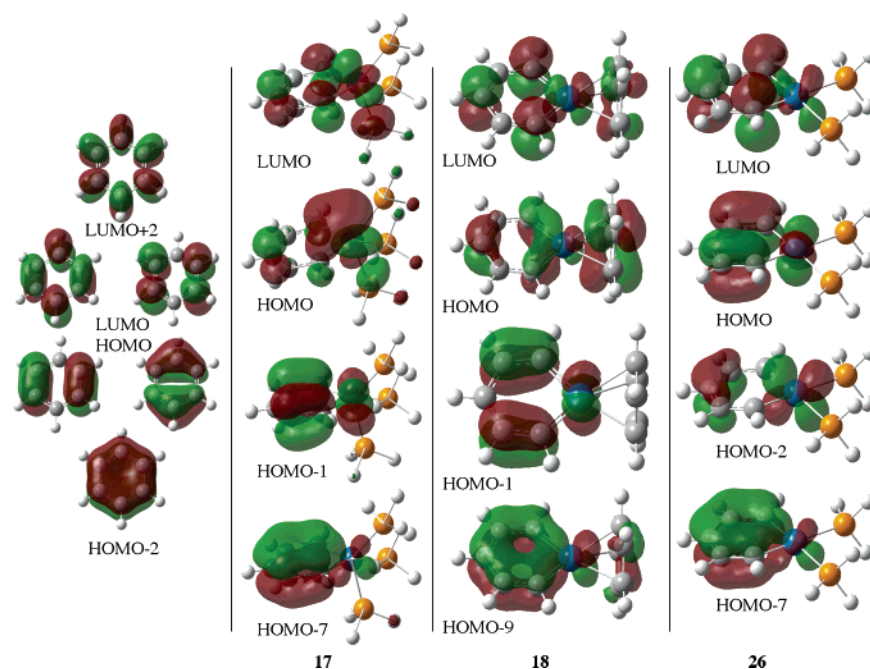


Figure 1. Selected molecular orbitals of benzene, iridiabenzene (C_5H_5Ir)(PH_3)₃ (**17**), and platinabenzene (C_5H_5Pt)Cp (**18**) and $[(C_5H_5Pt)(PH_3)_2]^+$ (**26**) complexes. Atomic color scheme: H, white; C, gray; P, yellow; metal, blue.

Table 1. NICS(x) ($x = 0.0, 1.0$, in ppm) and Magnetic Susceptibility Anisotropy ($\Delta\chi$, in cgs ppm) Values for Various Systems Studied

compound	NICS(1.0)	NICS(0.0)	$\Delta\chi$
benzene (C_6H_6)	-10.0	-7.7	-61.7
cyclobutadiene (C_4H_4 , D_{2h} symmetry)	+18.2	+27.5	+21.9
$(C_5H_5Ir)(PH_3)_3$ (17)	-8.8 ^a	-3.7	+93.9
<i>trans,cis</i> - $(C_5H_5Os)(PH_3)_2(CO)Cl$ (19)	-3.5	+2.5	-10.0
$(C_5H_5Pt)Cp$ (18)			
– metallabenzene ring	-6.4	-2.6	+43.2
– Cp ring	-7.9	-16.1	
$[(C_5H_5Pt)(PH_3)_2]^+$ (26)	+3.9	+9.1	+72.0
$[(C_5H_5Pt)(PH_3)_3]^+$ (28)	-5.5	-1.2	+60.0
$(C_5H_5Pt)(PH_3)_2(CH_3)$ (27)			
– syn to Me	-7.9	-6.5	+45.4
– anti to Me	-10.0		
$(C_5H_5Ir)(PH_3)_2Cl_2$ (20)	-3.2	+2.8	-22.7
<i>trans,cis</i> - $(C_5H_5Ru)(PH_3)_2(CO)Cl$ (23)	-3.2	+3.2	-43.35
$(C_5H_5Ru)Cp(CO)$ (22)			
– syn to CO	-6.0	+1.0	-46.6
– anti to CO	-1.0		
– Cp ring	-10.4	-19.8	
borazine ($B_3N_3H_6$, D_{3d} symmetry, 35)			-28.5 ^b
phosphaborabenzene ($B_3P_3H_6$, D_{3d} symmetry, 36)			-67.3 ^b

^a “Dummy” atom on face of ring opposite to the apical PH_3 ligand. ^b Based on CSGT-B3LYP/6-31G* values given in ref 96.

order and participating metal d -orbital may vary. One can clearly note the similarity between the two sets of MO's. The HOMO-3 of benzene, which has the well-recognized doughnut shape, is clearly the same as the lowermost of the shown MOs. Likewise, the metallabenzene HOMO and HOMO-1 (or HOMO-2) clearly resemble the degenerate HOMOs of benzene. Different metal d -orbitals have been observed participating in the aromatic MO's, including d_{z^2} , d_{xz} , and d_{yz} (the z -axis is defined as perpendicular to the plane of the ring, and the x -axis is defined as the $M-C_{para}$ axis). In fact, in the complexes where there is participation of the d_{z^2} orbital, often one lobe of the “dumbbell” and the torus, there is a slight deviation of the metal from the plane to allow for a better overlap.

The magnetic criterion of aromaticity is reflected in the ability of a system to sustain a diatropic ring current.⁸⁹ Schleyer introduced a computational method to evaluate how aromatic

or antiaromatic a system is. This method, termed nucleus-independent chemical shift (NICS), involves placing a dummy atom above the ring and calculating its NMR chemical shift.^{71,72,89} A negative NICS value indicates an aromatic system, while a positive value is obtained for antiaromatic systems. This was done here for benzene and a number of metallabenzene systems, and the negative values obtained for most systems show that these systems are indeed aromatic (Table 1). It has been demonstrated, however, that the magnitudes of NICS values do not reflect on the relative “aromaticity” of different systems, particularly when atoms of greatly different sizes are involved in the ring.^{89,91}

Another evaluation of the aromaticity of a system based on magnetic properties is the magnetic susceptibility anisotropy, $\Delta\chi$ (occasionally denoted as χ_{anis}).⁹⁷ This measure, obtained from the computed magnetic susceptibility tensor using eq 1 (see

Computational Details), was first proposed by Flygare.⁹⁷ Large negative values are expected for aromatic compounds. The $\Delta\chi$ values for a number of model metallabenzene complexes are listed in Table 1. The results obtained seem to cast some doubt on the aromaticity of metallabenzene complexes. Complex **23** seems to be the sole exception. Complex **20** cannot truly be considered aromatic according to this method as it is on par with **35**, which is not considered to be aromatic (vide infra). It should be noted that complexes **18** and **22** are not amenable to this method because they each contain two potentially aromatic rings, the metallabenzene and the Cp, that are perpendicular to each other.

The final criterion, reactivity, is more qualitative. Basically, a system has aromatic character if its reactivity resembles benzene's reactivity. Like benzene, **2** has been shown to undergo electrophilic aromatic substitution. The reaction of **2** with Fe/Br₂ or Cu(NO₃)₂/(CH₃CO)₂O results in bromination or nitration, respectively, *para* to the methylsulfide group, just as with MeSPh.⁴⁸ On the other hand, complexes **3**, **5**, and **6** easily undergo cycloaddition reactions with acetone, CO₂, CS₂, O₂, SO₂, nitrosobenzene (PhNO), and maleic anhydride.^{11,12} This cycloaddition reactivity is in sharp contrast to benzene's stability toward these reagents. The tendency of some metallabenzene to undergo Cp formation (vide infra) also strongly contrasts the aromatic nature of benzene.^{20,21,34,95,98–100}

This ambivalent aromatic nature of metallabenzene is somewhat similar to that of borazine (**35**, B₃N₃H₆). This compound has six equivalent B–N bonds and has been shown to undergo electrophilic substitution.^{101,102} It also has an aromatization stabilization energy, another measure of aromaticity, similar to phosphorabenzene (**36**, B₃P₃H₆).^{96,103} Nonetheless, it has been shown recently, based on NICS, $\Delta\chi$, and magnetic susceptibility exaltation (Λ) calculations, that **35** is actually not aromatic, whereas **36** is.^{72,96} The nonaromatic character of borazine (**35**) was explained by the large difference in electronegativity between nitrogen and boron that leads to localization of electron density on the nitrogen; in **36**, the difference is much smaller and permits greater electron delocalization.⁷² Furthermore, like metallabenzene, **35** tends to readily undergo addition reactions,¹⁰⁴ and the reported electrophilic substitution was the first such example.^{101,102}

It should, moreover, be noted that the applicability of NICS and $\Delta\chi$ calculations with metallabenzene has some limitations. The NICS(1.0) values, based on the chemical shift of the “dummy” atom, will be affected by close proximity to ligands on the metal center. Likewise, the magnetic susceptibility tensor, and hence $\Delta\chi$, will also be affected by the metal ligands and therefore will not solely be a measure of the ring aromaticity.

Table 2. Summary of Aromaticity Measures Used and the Results

method	parameter observed	aromatic?
geometry	ring planarity	yes
	ring bond length equalization	yes
	ring angle equalization	yes
molecular orbitals	aromatic MO delocalization	yes
		yes
magnetic properties	NICS	yes, with exceptions
	$\Delta\chi$	no, with exceptions
reactivity	cycloaddition chemistry	no
	electrophilic aromatic substitution	yes
	Cp formation	no

This is further complicated in complexes **18** and **22** where there is a Cp ring, a second, independent aromatic system, perpendicular to the metallabenzene ring. Chamizo et al. have previously determined that iridiabenzene **3** is not aromatic based on the absolute hardness $\tau = (E_{\text{LUMO}} - E_{\text{HOMO}})/2$ of the system, calculated at the extended Hückel level of theory.³⁸ Based on the abovementioned methods (Table 2), it is difficult to state with any certainty whether the metallabenzene complexes are truly aromatic or not.

Metallabenzene Formation. A. Osmabenzene (1). The reaction of acetylene with (Ph₃P)₃Os(CO)(CS) (**37**) resulted in the formation of the first metallabenzene (**1**).^{8,47} The mechanism of formation of **1** has yet to be explored. We examined the mechanism for the formation of the model complex ($\eta^3\text{-C,C,S-C}_5\text{H}_4\text{S}$)Os(PH₃)₂(CO) (**38**) from (PH₃)₃Os(CO)(CS) (**39**). The mechanism found is depicted in Scheme 3, and Figure 2 shows the reaction profile. The calculated C=C bond lengths and the reaction energetics are also shown in Scheme 3.

The reaction was found to proceed by the following mechanism. Initial phosphine dissociation (**40**) allows for η^2 -coordination of acetylene (**41**). As with alkenes, alkyne complexes involve a Dewar–Chatt–Duncanson-like resonance between an acetylene–metal(*n*) complex (**41a**) and a metallabenzene(*n*+2)–cyclopropene (**41b**).^{45,105,106} The C–C bond length calculated at 1.300 Å is closer to the C=C bond length in ethylene (calculated to be 1.344 Å) than to the C≡C bond in acetylene (calculated to be 1.211 Å). The next step involves migratory insertion (**42**) of the CS ligand into the metal–carbon σ -bond of the osmacyclopropene structure. The formation of an osmacyclobutadiene has been observed in a related system.¹⁰⁷ Prior to coordination of the second acetylene, the CO ligand migrates from the position *trans* to the C(=S) ring carbon to the *cis* position (**43**) lest the second acetylene inserts into the wrong Os–C bond and push the sulfur to the opposite side of the ring from the osmium. Coordination of a second acetylene (**44**) and subsequent C–C coupling would lead to a 2-osma-3,5-cyclohexadien-1-thione complex (**45**). Part of the large negative ΔG_{298} this reaction would be accounted for by the release of ring strain in going from a four- to a six-membered ring. The formation of the three-membered Os–C–S ring, to give the final product (**38**), proceeds via a reaction that can be described as either an intramolecular C=S oxidative addition or complete C=S bond coordination akin to formation of metallacyclopropanes by ethylene coordination. The formation

(94) Wu, H.-P.; Lanza, S.; Weakley, T. J. R.; Haley, M. M. *Organometallics* **2002**, *21*, 2824–2826.

(95) Jacob, V.; Weakley, T. J. R.; Haley, M. M. *Organometallics* **2002**, *21*, 5394–5400.

(96) Jemmis, E. D.; Kiran, B. *Inorg. Chem.* **1998**, *37*, 2110–2116.

(97) Flygare, W. H. *Chem. Rev.* **1974**, *74*, 653–687.

(98) Yang, J.; Jones, W. M.; Dixon, J. K.; Allison, N. T. *J. Am. Chem. Soc.* **1995**, *117*, 9776–9777.

(99) Ferde, R.; Allison, N. T. *Organometallics* **1983**, *2*, 463–465.

(100) Ferde, R.; Hinton, J. F.; Korfmacher, W. A.; Freeman, J. P.; Allison, N. T. *Organometallics* **1985**, *4*, 614–616.

(101) Chiavarino, B.; Crestoni, M. E.; Fornarini, S. *J. Am. Chem. Soc.* **1999**, *121*, 2619–2620.

(102) Chiavarino, B.; Crestoni, M. E.; Di Marzio, A.; Fornarini, S.; Rosi, M. *J. Am. Chem. Soc.* **1999**, *121*, 11204–11210.

(103) Haddon, R. C. *Pure Appl. Chem.* **1982**, *54*, 1129–1142.

(104) Cotton, F. A.; Wilkinson, G. *Advanced Inorganic Chemistry*; Series 5th ed.; John Wiley & Sons: New York, 1988.

(105) Dewar, M. J. S. *Bull. Soc. Chim. Fr.* **1951**, *18*, C71.

(106) Chatt, J.; Duncanson, L. A. *J. Chem. Soc.* **1953**, 2939.

(107) Elliott, G. P.; Roper, W. R. *J. Organomet. Chem.* **1983**, *250*, C5–C8.

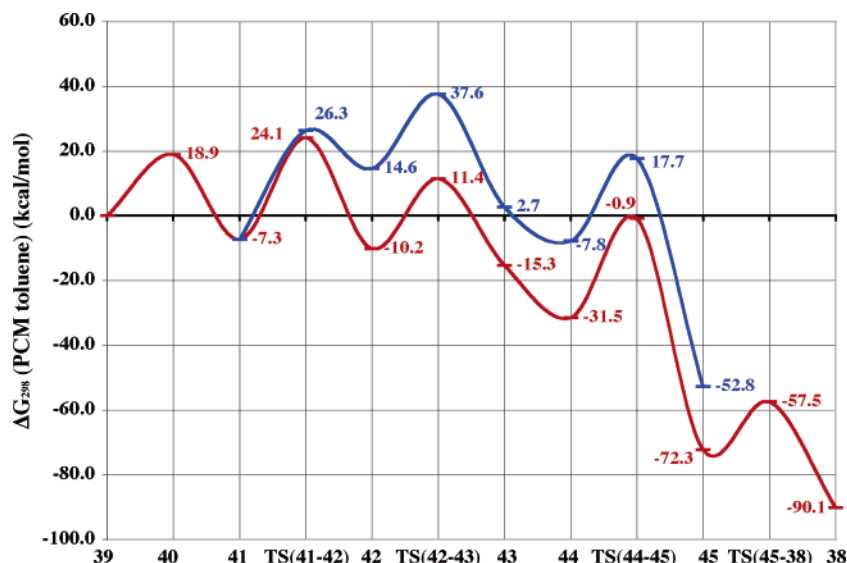
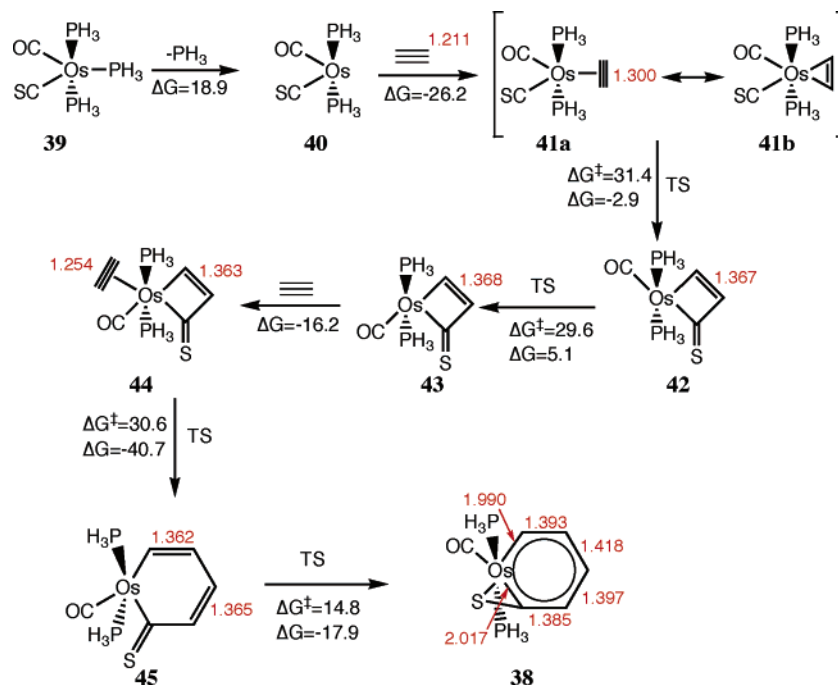


Figure 2. Reaction profile (ΔG_{298} , PCM(toluene)-mPW1K/SDB-cc-pVDZ//mPW1K/SDD, kcal/mol) for the formation of **38** (red) and the analogous reaction with CO, instead of CS, migratory insertion (blue). The compound labels refer to the CS migratory insertion route.

Scheme 3. Most Plausible Route to the Formation of **38**, the Computational Analogue of **1**,^{8,47} Including the Reaction Energies (ΔG_{298} , PCM(Toluene)-mPW1K/SDB-cc-pVDZ//mPW1K/SDD, kcal/mol) and C=C Bond Lengths (Å, in Red)



of an aromatic system would compensate for the ring strain associated with the formation of the Os–C–S three-membered ring annealed to the metallabenzene ring. The size of the sulfur atom probably also helps alleviate the ring strain.

Overall, this reaction (**39** + 2 HC≡CH → **38**) is fairly exergonic with $\Delta G_{\text{react},298} = -90.1$ kcal/mol. We solved the kinetic equations for this reaction and found that this is a pseudo-two-step reaction. The first barrier corresponds to the conversion of **39** into **40** with a height of $\Delta G_{298}^\ddagger = 18.9$ kcal/mol. The second step involves the conversion of **40** into **38**. The corresponding barrier, **TS(40–41)**, is $\Delta G_{298}^\ddagger = 31.4$ kcal/mol. Although this would seem too high for the fast reaction involved, one must remember that the PPh₃ ligands in **37** are replaced by

PH₃ ligands. Moreover, the reaction vessel is pressurized with acetylene, which is, therefore, present in a large excess, and this will drive the reaction.

An alternate route involving CO migratory insertion, instead of CS, was also considered and is included in Figure 2 (blue line). This leads to a rate-determining barrier, corresponding to migratory insertion and trans–cis CS migration, that is considerably higher ($\Delta G_{298}^\ddagger = 37.6$ kcal/mol). This possibly reflects the stronger Os–CS bond,¹⁰⁴ apparent in the relative bond lengths in **41** (Os–CO, 1.913 Å; Os–CS, 1.866 Å). Moreover, the formation of a three-membered Os–C–O ring does not occur, and the final product is the osma-3,5-cyclohexadienone complex. The oxygen atom is probably too small, compared to

Table 3. Calculated Atomic Polar Tensor (APT) and Natural Population Analysis (NPA) Charges of the Metal Atom in Various Calculated Metallabenzenes

complex	APT charge	NPA charge
(C ₅ H ₅ Ir)(PH ₃) ₃ (17)	-1.07	-0.03
(C ₅ H ₅ Pt)(η ⁵ -Cp) (18)	+0.08	+0.65
<i>trans,cis</i> -(C ₅ H ₅ Os)(PH ₃) ₂ (CO)Cl (19)	-1.12	-0.24
<i>trans,cis</i> -(C ₅ H ₅ Ir)(PH ₃) ₂ Cl ₂ (20)	-0.17	+0.19
[(C ₅ H ₅ Pt)(PH ₃) ₂] ⁺ (26)	-0.15	+0.31
[(C ₅ H ₅ Pt)(PH ₃) ₃] ⁺ (28)	-0.22	+0.41

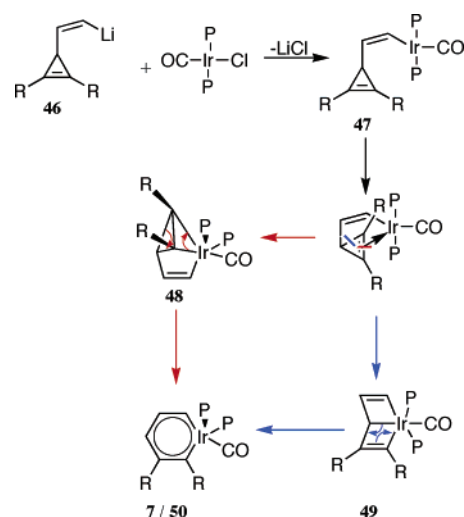
sulfur, to sufficiently relieve the ring strain. This process is a clear example where the identity of a heteroatom (S vs O) controls the outcome of metal complex formation.

Likewise, a reaction mechanism where CS migratory insertion follows, rather than precedes, coupling with the second acetylene was ruled out. In the primary route, migratory insertion vacates a metal coordination site to allow for coordination of the second acetylene. In this alternate route, phosphine dissociation would be required to avoid the formation of 20-electron complexes. Thus, such a route is much less plausible. Furthermore, the kinetic equations for such a mechanism indicate a pseudo-two-step reaction with barriers of $\Delta G^{\ddagger}_{298} = 18.9$ and 38.6 kcal/mol.

B. X-ray Photoelectron Spectroscopy Measurements. The X-ray photoelectron spectroscopy (XPS) Os(4f_{7/2}) binding energies for the osmium centers in **1** (51.0 eV) and **2** (51.2 eV) are in the range for Os(II). (See Supporting Information for the full set of XPS data and literature values for different osmium formal oxidation states, Tables S6 and S7.) To the best of our knowledge, there are not any XPS data available on similar osmium organometallic complexes for comparison. Most literature complexes are coordination complexes with halide or outersphere counteranions. This leads to a better separation of charges and thus better “defined” oxidation states. Alkyl and hydride ligands are assigned negative charges in the definition of the formal metal oxidation state, even if formalism and reality differ. In fact, the actual charge on a hydride or alkyl ligand can be neutral or even cationic. For example, certain metal hydrides, even though formally -1, are actually acidic.^{108–111} One would thus expect XPS in these cases to give an oxidation state lower than expected, as has been observed, for instance, for an iron(II) hydride.¹¹² In the case of the metallabenzenes, the situation is even more complicated where the organic fragment can accept charge, evident from the calculated atomic polar tensor (APT) and natural population (NPA) charges of various model metallabenzenes (Table 3). In addition, the XPS signal for S(2p_{3/2}) in **1** at 162.2 eV indicates a highly reduced sulfur center, consistent with an RS⁻ ligand in the reaction mechanism found for the synthesis of **1** (Scheme 3). The well-resolved NMR spectra of **1** and **2**^{8,48} clearly indicate that they are diamagnetic complexes and rule out the assignment of paramagnetic Os(I) or Os(III) systems.

C. Metallabenzenes 7 and 8. The Ir (**7**) and Pt (**8**) metallabenzenes were obtained by reacting metal halide salts with 2,3-diphenylcyclopropenylvinyl lithium (**46**) (Scheme

Scheme 4. Potential Routes to **7** and **50**^a



^a In the experimental system (**7**), R = Ph and P = PMe₃.^{17–19} In the computational system (**50**), R = H, Me and P = PH₃. Complexes of type **7** and **48** with different R groups have been characterized by X-ray crystallography.^{17–20}

4).^{17–21,94,95} Two possible reaction mechanisms were proposed, one involving a metallabenzvalene intermediate (**48**) and the other involving a metalla-Dewar benzenelike structure (**49**) (Scheme 4).¹⁸ We examined these two possible routes here using the model system where the ring phenyl substituents are replaced with hydrogens or methyls and PH₃ ligands are used in lieu of PMe₃.

First we used the model system where the two phenyl groups on the cyclopropene ring were replaced by hydrogens. The reaction profile found is shown in Figure 3 (blue). After ligand substitution, a cyclopropenylvinyliridium complex (**47**) is obtained. Two isomers were found, one where the cyclopropene ring points away from the iridium center (**47a**) and the other where it points toward it (**47b**); the former is slightly lower in energy by $\Delta G_{298} = 1.8$ kcal/mol. The transition state for the conversion of **47b** to the iridiabenzvalene complex (**48**), **TS(47b–48)**, was found and leads to a very low reaction barrier of $\Delta G^{\ddagger}_{298} = 1.7$ kcal/mol. Likewise, the transition state, **TS(48–50)**, for the formation of the iridiabenzene (**50**) was found. This transition state involves twisting of the C–C bond in the iridiacyclopropane ring to give the planar metallabenzene ring and results in a reaction barrier of $\Delta G^{\ddagger}_{298} = 39.5$ kcal/mol. Note, however, that the transition state is only 16.4 kcal/mol above **47a**, and these energies do not include the energy released during the initial ligand substitution reaction. We also examined the system with a 2,3-dimethylcyclopropenylvinyl ligand (Figure 3, green) and found only minor changes in the reaction profile.

The second route (Figure 3, red) involves C–C activation of the cyclopropene ring to give the iridia-Dewar benzene complex (**49**). While this intermediate, and the transition state leading to the metallabenzene complex, **TS(49–50)**, could be found, the transition state for its formation, **TS(47b–49)**, remained elusive. Nonetheless, the Dewar-benzene intermediate (**49**) is much higher in energy than both the iridiabenzvalene complex (**48**) ($\Delta G^{\ddagger}_{298} = 38.3$ kcal/mol) and even the transition state **TS(47b–48)** leading to it. Likewise, the transition state, **TS(49–50)**, leading to the metallabenzene (**50**) from the iridia-Dewar benzene (**49**) is also much higher than its iridiabenz-

(108) Hieber, W.; Wagner, G. Z. *Naturforsch.* **1958**, *13B*, 339–347.

(109) Hieber, W.; Hübel, W. Z. *Elektrochem.* **1953**, *57*, 235–243.

(110) Galembeck, F.; Krumholz, P. *J. Am. Chem. Soc.* **1971**, *93*, 1909–1913.

(111) Walker, H. W.; Kresge, C. T.; Ford, P. C.; Pearson, R. G. *J. Am. Chem. Soc.* **1979**, *101*, 7428–7429.

(112) Bianchini, C.; Masi, D.; Peruzzini, M.; Casarin, M.; Maccato, C.; Rizzi, G. A. *Inorg. Chem.* **1997**, *36*, 1061–1069.

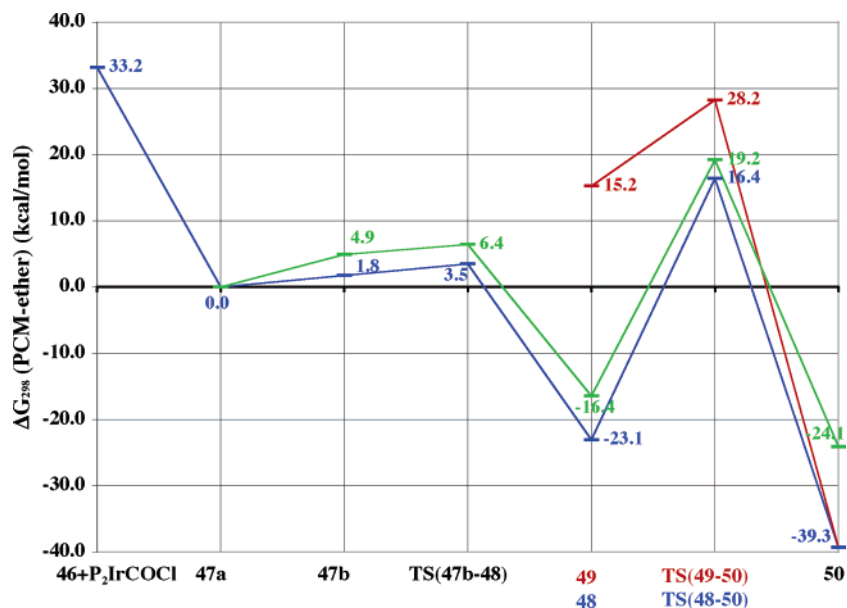


Figure 3. Reaction profiles ($\Delta G_{298}^{\ddagger}$, PCM(ether)-mPWIK/SDB-cc-pVDZ//mPWIK/SDD, kcal/mol) for the formation of **50** via **48** (blue) or **49** (red). Also included is the dimethyl system (green, see text).

valene counterpart. It would thus appear that the first route is more plausible, especially since a number of iridiabenzvalene complexes were isolated and characterized by X-ray crystallography.^{18,19}

As the formation of **8** and **26** involved a similar synthesis, it is also reasonable to assume that the platinum analogues follow a similar reaction pathway. The formation of **8**, however, would proceed twice through the route, once to form the Cp ring and again to form the metallabenzene. In the case of the formation of $[(C_5H_5Pt)(PH_3)_2]^+$ (**26**), the barrier for the conversion of the platinabenzvalene to the platinabenzene was found to be $\Delta G_{298}^{\ddagger} = 16.1$ kcal/mol and the reaction is exergonic by $\Delta G_{298} = -20.6$ kcal/mol. Unlike iridium, a platinum analogue of **47** could not be found. These results are fully in agreement with the conclusions drawn by Haley.^{17–21,94,95}

Metallabenzene Stability and Reactivity. A. Cyclopentadienyl Complex Formation. One common reaction of metallabenzenes is the formation of cyclopentadienyl (Cp) complexes.⁴² This was demonstrated by Jones and Allison⁹⁸ in an experiment where they prepared at -50 °C a ruthenabenzene, (3,5-Ph₂-2-OEt-C₅H₂Ru)(CO)(η^5 -Cp) (**51**), and then observed its conversion at -30 °C by NMR to the related Cp₂Ru complex. This clearly established the intermediacy of metallabenzenes in the formation of Cp complexes. In a similar reaction with rhenium and iron systems, Cp complexes were obtained instead of the expected rhenabenzene⁹⁹ and ferrabenzene.¹⁰⁰ In addition, Cp complexes of iridium⁹⁴ and platinum⁹⁵ were obtained in reactions that in other systems yielded metallabenzene complexes.^{17,19–21}

This is a very unusual C–C coupling reaction in that one six-membered aromatic system is converted into another five-membered aromatic system via a nonaromatic transition state. Table 4 lists the reaction energies and barrier heights found. The reaction proceeds via an asymmetric transition state where there is a clear pattern of alternating short and long bonds, strongly resembling one of the two Kekulé structures (Scheme 1). This would indicate that the reaction may be classified as a carbene migratory insertion.⁴⁶ In the transition state, the two ortho carbons are pinched toward each other and the ring

planarity is lost. Figure 4 depicts three examples of the transition state for Cp formation; all the others have similar features. This reaction proceeds in the same manner for all the metallabenzenes studied and is independent of the metal and ligand environment. This leads to a Cp complex, which may then lose a ligand and/or undergo Cp ring slippage to lead to the final product.

One commonality with regard to the molecular orbitals was observed for all reactive complexes and another for all the stable complexes. The HOMOs of benzene are degenerate and have one nodal plane (Figure 1). In the metallabenzene complexes, this degeneracy is lifted and these two orbitals have different energies. In the reactive complexes, the HOMO has the nodal plane passing through the M–C_{para} axis, while, in the stable complexes, this plane transects the two C_{ortho}–C_{meta} bonds. The nature of this difference is not readily apparent. The symmetry of the HOMO was also a key factor in the cycloaddition reactivity.^{40,41} If one were to consider the hypothetical cycloaddition reactivity of the metallabenzenes unstable toward Cp formation, such a change in the symmetry of the HOMO would have a dramatic impact on the reactivity making the 1,2 instead of 1,4 cycloaddition symmetry favored.

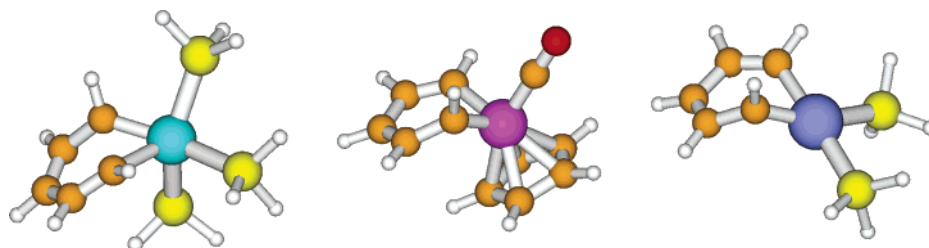
Based on this model system (vide supra), one cannot determine whether a redox or nonredox mechanism for Cp formation is more plausible. To that end, we took a representative series of metallabenzenes (**17–20**, **26**, **28**, **30**, **31**) and substituted the C_{para} with either an electron-donating (NH₂) or -withdrawing (NO₂) group. It is known that electron-donating groups (EDG) stabilize, and electron-withdrawing groups (EWG) conversely destabilize, higher oxidation states. If the Cp formation was to occur via a nonredox migratory insertion, then the stabilization afforded by the EDG (and the destabilization by the EWG) to the metallabenzene reactant and the Cp product would be similar and the reaction barrier would not be greatly affected. However, if the reaction proceeded by a reductive elimination pathway, then a major impact on the reaction barrier height would be observed.

Table 5 compares the Cp formation barrier heights and reaction energies for the above series of *para*-substituted (R =

Table 4. Calculated Reaction and Barrier Height Energies ($\Delta G_{298}^{\ddagger}$, PCM(Ether)-mPW1K/SDB-cc-pVDZ//mPW1K/SDD, kcal/mol) for the Various Cp Formation Reactions Studied

	TS	initial product		final product ^a		ref ^b
(C ₅ H ₅ Ir)(PH ₃) ₃ (17)	44.4	(η^1 -Cp)Ir(PH ₃) ₃	-12.5	(η^5 -Cp)Ir(PH ₃) ₂	-25.0	12
(C ₅ H ₅ Pt)(η^5 -Cp) (18)	45.9	(η^3 -Cp) ₂ Pt	-2.9			20, 21
<i>trans,cis</i> -(C ₅ H ₅ Os)(PH ₃) ₂ (CO)Cl (19)	27.7	<i>trans</i> -(η^1 -Cp)Os(PH ₃) ₂ - (CO)(Cl) ^c	-9.4	<i>cis</i> -(η^1 -Cp)Os(PH ₃) ₂ - (CO)(Cl) ^d	-16.3	8
<i>trans,cis</i> -(C ₅ H ₅ Ir)(PH ₃) ₂ Cl ₂ (20)	35.2	<i>trans,cis</i> -(η^3 -Cp)Ir(PH ₃) ₂ Cl ₂	10.2 ^e	(η^5 -Cp)Ir(PH ₃)Cl ₂	-15.3	12
<i>trans,cis</i> -[(C ₅ H ₅ Ir)(PH ₃) ₂ (CH ₃ CN)] ²⁺ (21)	37.2 ^f	<i>trans,cis</i> -[(η^1 -Cp)Ir(PH ₃) ₂ - (CH ₃ CN)] ²⁺	10.5 ^g	[(η^5 -Cp)Ir(PH ₃) ₂ - (CH ₃ CN)] ²⁺	-24.1 ^h	12
(C ₅ H ₅ Ru)(η^5 -Cp)(CO) (22)	25.2 ⁱ	(η^3 -Cp)Ru(CO)(η^5 -Cp)	-18.4 ⁱ			98
<i>trans,cis</i> -(C ₅ H ₅ Ru)(PH ₃) ₂ (CO)Cl (23)	24.6	<i>trans</i> -(η^1 -Cp)Ru(PH ₃) ₂ - (CO)(Cl) ^c	-19.0			
(C ₅ H ₅ Fe)(η^5 -Cp)(CO) (24)	19.2	(η^1 -Cp)Fe(CO)(η^5 -Cp)	-31.0	(η^5 -Cp) ₂ Fe	-66.4	99
<i>mer</i> -(C ₅ H ₅ Re)(PH ₃)(CO) ₃ (25)	24.1	<i>mer</i> -(η^1 -Cp)Re(PH ₃)(CO) ₃	-30.3	(η^5 -Cp)Re(CO) ₃	-63.4	100
[(C ₅ H ₅ Pt)(PH ₃) ₂] ⁺ (26)	24.0	[(η^5 -Cp)Pt(PH ₃) ₂] ⁺	-37.5			95
(C ₅ H ₅ Pt)(PH ₃) ₂ (<i>apical</i> -CH ₃) (27)	32.6	(η^1 -Cp)Pt(PH ₃) ₂ (CH ₃)	-41.8			
[(C ₅ H ₅ Pt)(PH ₃) ₃] ⁺ (28)	34.9	[(η^1 -Cp)Pt(PH ₃) ₃] ⁺	-34.4	[(η^5 -Cp)Pt(PH ₃) ₂] ⁺	-36.6	
(C ₅ H ₅ Rh)(PH ₃) ₃ (29)	20.5 ^j	(η^5 -Cp)Rh(PH ₃) ₂	-56.8			
(C ₅ H ₅ Rh)(PH ₃) ₂ (30)	33.4	(η^3 -Cp)Rh(PH ₃) ₃	-20.3	(η^5 -Cp)Rh(PH ₃) ₂	-45.6	
<i>trans,cis</i> -(C ₅ H ₅ Rh)(PH ₃) ₂ Cl ₂ (31)	32.1	<i>trans,cis</i> -(η^3 -Cp)Rh(PH ₃) ₂ Cl ₂	-3.2			
(C ₅ H ₅ Pd)(η^5 -Cp) (32)	33.8	(η^3 -Cp) ₂ Pd	-24.3			
[(C ₅ H ₅ Pd)(PH ₃) ₂] ⁺ (33)	19.1	[(η^5 -Cp)Pd(PH ₃) ₂] ⁺	-54.2			
[(C ₅ H ₅ Pd)(PH ₃) ₃] ⁺ (34)	23.6	[(η^1 -Cp)Pd(PH ₃) ₃] ⁺	-46.2	[(η^5 -Cp)Pd(PH ₃) ₂] ⁺	-56.0	

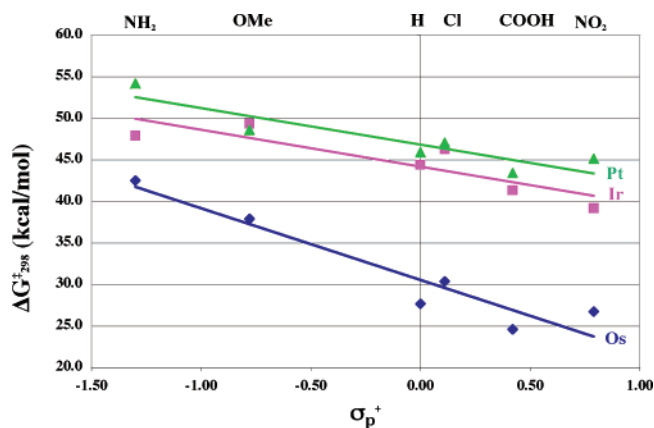
^a Overall reaction energy for the cases where there is a second step after Cp formation. ^b References of experimental systems modeled where applicable. ^c Square pyramidal geometry. ^d Trigonal bipyramidal geometry. ^e A *cis,trans* isomer was found with an overall reaction energy of 7.1 kcal/mol. ^f Calculation in CH₃CN rather than ether as in experimental system. ^g A *cis,trans* isomer was found with an overall reaction energy of 4.1 kcal/mol. ^h Loss of PH₃ instead of CH₃CN would lead to an overall reaction energy of -15.1 kcal/mol. ⁱ Calculation in CH₂Cl₂ rather than ether as in experimental system. ^j Initial phosphine dissociation from **30** has a calculated reaction energy of $\Delta G_{298}^{\ddagger} = 11.2$ kcal/mol leading to an overall barrier of $\Delta G_{298}^{\ddagger} = 31.7$ kcal/mol.

**Figure 4.** Geometry of the transition states for Cp formation from complexes **17** (left), **24** (center), and **26** (right). Atomic color scheme: H, white; C, orange; P, yellow; Ir, turquoise; Fe, purple; Pt, blue.**Table 5.** Reaction Energies and Barrier Heights ($\Delta G_{298}^{\ddagger}$, PCM(Ether)-mPW1K/SDB-cc-pVDZ//mPW1K/SDD, kcal/mol) for Cp Formation in Various *para*-Substituted Metallabenzenes

metallabenzene	$\Delta G_{298}^{\ddagger}$			$\Delta G_{298}^{\ddagger}$ (first step)			$\Delta G_{298}^{\ddagger}$ (overall) ^a		
	NH ₂	H	NO ₂	NH ₂	H	NO ₂	NH ₂	H	NO ₂
17	47.9	44.4	39.2	-5.4	-12.5	-15.8			
18	54.2	45.9	45.1	1.8	-2.9	-5.3			
19	42.5	27.7	26.7	8.0	-9.4	-12.4	-11.8	-16.3	-12.4
20	51.0	35.2	32.5	10.3	10.2	4.5	5.7	7.1	0.0
26	45.8	24.0	18.6	-8.5	-37.5	-42.3			
28	44.0	34.9	34.4	-15.8	-34.4	-39.4	-17.9	-36.6	-39.1
30	35.3	33.4	24.3	-20.4	-20.3	-36.0			
31	49.4	24.6	28.3	-2.5	-19.0	-11.7			
28 → 26 + P	36.4	24.9	21.8	-17.9	-36.6	-39.1			

^a For the cases where there is a second step after Cp formation.

H, NH₂, NO₂) metallabenzenes. One can clearly observe that the order of stability, in all cases, is NH₂ > H > NO₂. The effects of EDG substitution are generally more dramatic than EWG substitution and in certain cases are even more than 15 kcal/mol. Clearly, these results support a reductive elimination process.¹¹³ For complexes **17**–**19**, an additional three substituents (Cl, COOH, and OMe) were used and a somewhat linear relationship was found between the Cp formation barrier height ($\Delta G_{298}^{\ddagger}$) and σ_p^+ (Figure 5).¹¹⁴ While the correlation is not

**Figure 5.** Hammett plot ($\Delta G_{298}^{\ddagger}$ vs σ_p^+) for the Cp formation from *para*-substituted analogues of **17** (Ir, magenta), **18** (Pt, green), and **19** (Os, blue).

perfect ($R^2 = 0.78$ (Ir), 0.82 (Pt), and 0.90 (Os)), the trends are quite apparent.

One may wonder whether Cp complexes may be used as starting complexes in the formation of metallabenzenes. While the Cp complexes are generally the thermodynamic products, we have demonstrated that the kinetics, and to a lesser extent

(113) Cohen, R.; van der Boom, M. E.; Shimon, L. J. W.; Rozenberg, H.; Milstein, D. *J. Am. Chem. Soc.* **2000**, *122*, 7723–7734.

(114) March, J. *Advanced Organic Chemistry*, 3rd ed.; John Wiley & Sons: New York, 1985; p 224.

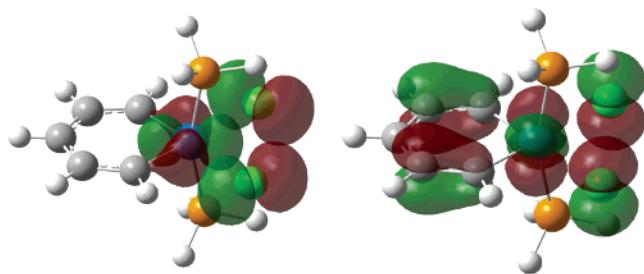


Figure 6. HOMO (left) and HOMO-1 (right) of complex **20**, *trans,cis*-(C₅H₅Ir)(PH₃)₂Cl₂.

the thermodynamics, of the reaction can be shifted by adding electron donor or acceptors groups to the ring. With the right substitution pattern on the Cp ring and the proper reaction conditions, this might be possible. This suggestion is not as far-fetched as it may seem after Xi and Takahashi et al. prepared benzene and pyridine derivatives from 1-titanocene-2,4-cyclopentadiene complexes and benzonitrile and clearly demonstrated that one of the Cp rings is split 2:3 between the two products under mild homogeneous reaction conditions.^{115,116}

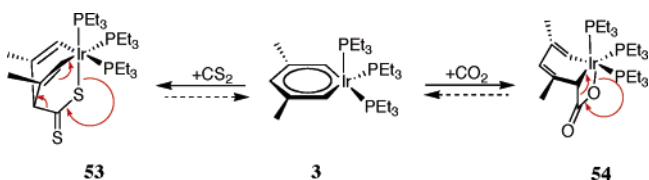
One metallabenzene that was found to be surprisingly stable is complex **4**, which has been characterized by X-ray crystallography.¹² An examination of its computational analogue (**20**) reveals an explanation for its stability. It has been observed that the frontier molecular orbitals (FMO's) are key in determining the reactivity of a compound. The HOMO of **20** (Figure 6) is an Ir–Cl₂ π* orbital and has little or no participation of the ring fragment; the HOMO-1 orbital also has, in addition to participation of the ring fragment, considerable Ir–Cl₂ π* nature. This would impact the stability of the complex. Furthermore, this complex would be stabilized by the π-donating ability of the Cl ligands.

B. Formal Metal Oxidation State. With respect to the formal metal oxidation state in the osmabenzene **1**, following the reaction (Scheme 3) leads to the following conclusions. The final step is the conversion of the formally Os(II) 2-osma-3,5-cyclohexadien-1-thione complex (**44**) to the osmabenzene (**38**). This can be considered either oxidative addition or full donation of the C=S bond, akin to alkene coordination.

The formation of the iridiabenzene (**50**) from the iridiabenzvalene (**48**) involves reorganization of the carbon skeleton (Scheme 4). Overall, the iridium center has the same number of bonds, and there is no apparent net change in the electron count on the metal center. This would also hold even if the Dewar benzene intermediate was actually involved. Thus, the reaction would appear to be nonredox, and the iridiabenzene would formally be an Ir(III) complex. Likewise, complex **8** would formally be a Pt(IV) complex. This is in agreement with the reported syntheses of iridiabenzenes **3**¹² and **10** (**11**) (Scheme 1)²² and by the demonstration by Hughes et al. that an iridiabenzene is involved in the rearrangement of an iridiacyclohexadiene.^{35,36}

It is noteworthy that the reaction that is expected to yield [(1,2-Ph₂C₅H₃Pt)(PEt₃)₂]⁺ (**52**) led instead to Cp products,⁹⁵ while (1,2-Ph₂C₅H₃Pt)(1,2-Ph₂Cp) (**8**) was successfully prepared.²⁰ Metallabenzenes **52** and **8** are 16- and 18-electron complexes, respectively. If they are low valent, formally Pt(II)

Scheme 5. Cycloaddition Reactions of CS₂ and CO₂ with Iridiabenzene **3**^{12 a}



^a Shown is the mechanism of the hypothetical reverse reaction.

complexes, then it is unexpected that **52** would be unstable while **8** was isolated. However, a 16-electron coordinatively unsaturated Pt(IV) complex is expected to be unstable.

Our computational study into the cycloaddition reactivity of metalloaromatic compounds has been previously reported.^{40,41} The cycloaddition products obtained with **3** are formally Ir(III) complexes as they bear two vinyl (or one vinyl and one alkyl) and one alkoxy or sulfide ligands. This reaction, as shown in Scheme 5, does not appear to be a redox reaction, and the substrates, acetone, CO₂, CS₂, maleic anhydride, SO₂, O₂, or PhNO are generally not reducing agents. The reaction consists of a reordering of the chemical bonds, and the iridium center before and after the reaction has the same number of chemical bonds and there is not a net change in the electron count at the metal center.

Summary and Conclusions

A detailed mechanistic investigation into the chemistry of metallabenzenes is presented and the question of aromaticity in metallabenzenes was examined. Metallabenzenes have planar geometries with bond length equalization, and have molecular orbitals that are akin to those of benzene. The NICS values indicate that some metallabenzenes may be aromatic although the Δχ values are less supportive (Table 1). Nevertheless, other issues, such as the presence of metal ligands and, in certain cases other independent aromatic systems (Cp ligands), may make the applicability of these two latter methods to organometallic compounds questionable. Moreover, although electrophilic substitution has been observed,⁴⁸ the cycloaddition chemistry is more prevalent.¹²

The mechanism for the formation of the osmabenzene **1** was elucidated (Scheme 3, Figure 2). In the model system, it was found that the reaction pathway involves phosphine dissociation, η²-coordination of the first acetylene molecule followed by C–C coupling to give osmacyclobutenthianone complex (**42**). From this complex, CO migration to the other *cis*-coordination site, η²-coordination of the second acetylene followed by C–C coupling, and C=S activation of the resulting osmacyclohexadienthione complex (**45**) yield in the end the osmabenzene (**38**). This pseudo-two-step reaction is fairly exergonic with barrier heights of ΔG[‡]₂₉₈ = 18.9 and 31.4 kcal/mol.

The formation of iridiabenzene **50** and platinabenzene **26** was also examined (Scheme 4, Figure 3). It was found that this route involves the formation of a metallabenzvalene structure (**48**), which rearranges to give the metallabenzene complexes.

The cyclopentadienyl formation reactivity was examined in depth (Table 4). The transition state for this reaction (Figure 4) is asymmetric and resembles the Kekulé benzene structure. It was found that substitution of the ring *para*-carbon with electron donating groups stabilizes the system (Table 5). The metallabenzenes are kinetic rather than thermodynamic products.

(115) Xi, Z.; Sato, K.; Gao, Y.; Lu, J.; Takahashi, T. *J. Am. Chem. Soc.* **2003**, *125*, 9568–9569.

(116) Kempe, R. *Angew. Chem., Int. Ed.* **2004**, *43*, 1463–1464.

One key issue hitherto unresolved is the formal metal oxidation state of the metallabenzene complexes. They all lie on a continuum between a low valent Fischer carbene complex with a four electron $C_5R_5^-$ moiety and a high valent Schrock carbene (alkylidene) complex with a six-electron $C_5R_5^{3-}$ fragment. An examination of the formation, reactivity, and stability of the different metallabenzenes suggests that the high valent formalism is more plausible.

Acknowledgment. Research was supported by the Helen and Martin Kimmel Center for Molecular Design, the Minerva Foundation (Munich, Germany), the German Federal Ministry for Education and Research (BMBF), and by grants from Sir Henry Djanogly, CBE, and the Henry Gutwirth Fund for the Promotion of Research. J.M.L.M. is a member of the Lise Meitner-Minerva Center for Computational Quantum Chemistry. M.E.vdB. is the head of the Minerva Junior Research Group

(M.J.R.G.) for Molecular Materials and Interface Design and the incumbent of the Dewey David Stone and Harry Levine Career Development Chair, and thanks the Israeli Council of Higher Education for an Alon fellowship. M.A.I. acknowledges the Feinberg Graduate School of the Weizmann Institute of Science for a Ph.D. fellowship. The authors would like to thank Prof. Delano Chong (University of British Columbia) for providing a copy of his basis set completeness profile program.

Supporting Information Available: Cartesian coordinates of all calculated structures, f -polarization and diffuse $spdf$ functions of the aug-SDB-cc-pVDZ basis set (Table S2), and Tables S1–S7. This material is available free of charge via the Internet at <http://pubs.acs.org>.

JA047125E